*Biochimica et Biophysica Acta*, 1058 (1991) 363–373

*ADONIS* 000527289100170L

BBABIO 43345



# Orientation and linear dichroism of *Mastigocladus laminosus* phycocyanin trimer and *Nostoc* sp. phycocyanin dodecamer in stretched poly(vinyl alcohol) films.

Laura J. Juszczak [1], Barbara A. Zilinskas [2], Nicholas E. Geacintov [1], Jacques Breton [3] and Kenneth Sauer [4]

[1] *Chemistry Department, New York University, New York, NY (U.S.A.),* [2] *Department of Biochemistry and Microbiology, Cook College, Rutgers University, New Brunswick, NJ (U.S.A.),* [3] *Service de Biophysique, Departement de Biologie, C.E.N. de Saclay, Gif sur Yvette (France) and* [4] *Chemistry Department and Chemical Biodynamics Laboratory, Lawrence Berkeley Laboratory, University of California, Berkeley, CA (U.S.A.)*

(Received 30 May 1990)
(Revised manuscript received 7 November 1990)

Key words: Linear dichroism; Exciton model; Phycocyanin

**The linear dichroism (LD) spectra of the C-phycocyanin (C-PC) trimer disks oriented in poly(vinyl alcohol) films (PVA) at room temperature and at 95 K were determined. Utilizing the known atomic coordinates of the chromophores (Schirmer, T., Bode, W. and Huber, R. (1987) J. Mol. Biol. 196, 677–695) and theoretical estimates of the orientations of the transition dipole moments relative to the molecular framework, the LD spectra were simulated using the pairwise exciton interaction model of Sauer and Scheer (Biochim. Biophys. Acta 936 (1988) 157–170); in this model, the $\alpha$84 and $\beta$84 transition moments are coupled by an exciton mechanism, while the $\beta$155 chromophore remains uncoupled. Linear dichroism spectra calculated using this *exciton* model, as well as an uncoupled chromophore (*molecular*) model, were compared with experimental LD spectra. Satisfactory qualitative agreement can be obtained in both the *exciton* and *molecular* models using somewhat different relative values of the theoretically estimated magnitudes of the $\beta$155 oscillator strength. Because the relative contributions of each of the chromophores (and thus exciton components) to the overall absorption of the C-PC trimer are not known exactly, it is difficult to differentiate successfully between the *molecular* and *exciton* models at this time. The linear dichroism spectra of PC dodecamers derived from phycobilisomes of *Nostoc* sp. oriented in stretched PVA films closely resemble those of the C-PC trimers from *Mastigocladus laminosus*, suggesting that the phycocyanin chromophores are oriented in a similar manner in both cases, and that neither linker polypeptides nor the state of aggregation have a significant influence on these orientations and linear dichroism spectra. The LD spectra of oriented phycocyanins in stretched PVA films at low temperatures (95 K) appear to be of similar quality and magnitude as the LD spectra of single C-PC crystals (Schirmer, T. and Vincent, M.G. (1987) Biochim. Biophys. Acta 893, 379–385).**

## Introduction

Phycobilisomes (PBsomes) are supramolecular aggregates of pigment-protein complexes which harvest light energy in cyanobacteria and red algae (for review, see, for example, Ref. 1). The chromophores are bilins, linear tetrapyrroles which are covalently bound to the apoproteins via thioether bonds. Recently, the three-dimensional structures of C-phycocyanin (C-PC) disk-like structures derived from *Mastigocladus laminosus* and *Agmenellum quadruplicatum* (devoid of linker polypeptides) have been determined by X-ray analysis [2,3]. The orientations of the transition dipole moments of the chromophores have been estimated from the known atomic coordinates [3], and the available X-ray structural information has been employed to interpret

Correspondence: N.E. Geacintov, Chemistry Department, New York University, New York, NY 10003.

the absorption properties [4,5], fluorescence polarization [4], energy transfer, and exciton coupling characteristics [6,7], in these C-PC trimeric aggregates.

Polarized light optical spectroscopy techniques using samples oriented with respect to a laboratory axis can also provide valuable information on the orientation of chromophores in photosynthetic systems [8], although, obviously, with less detail than is obtained by high-resolution X-ray diffraction techniques. However, optical methods such as the linear dichroism technique [8] are simpler, and non-crystalline samples of various dimensions and degrees of aggregation, including whole cells, can be studied in aqueous suspensions or in other media.

Whole cells and intact PBsomes suspended in aqueous buffer solutions can be easily oriented by the hydrodynamic flow gradient-forces in Couette cells [9]. PBsome subunits, e.g., the C-PC trimers, cannot be oriented sufficiently using this hydrodynamic flow dichroism approach because of the increased Brownian rotational motions of these smaller particles. However, linear dichroism studies on PBsomes and even smaller particles have been carried out using electric field pulses [10–12], sucrose-gelatin gel [13], polyacrylamide gel [14,15], and gelatin gel [9] squeezing methods. Frackowiak and co-workers have extensively studied the spectroscopic properties of PBsomes and their subunits in stretched poly(vinyl alcohol) (PVA) films [16,17]. Recently, the polarized absorption spectra of thin single crystals of C-PC trimers of *M. laminosus* have been investigated [18].

In this paper, the linear dichroism (LD) spectra of C-PC trimers derived from *M. laminosus* oriented in stretched PVA films measured at 296 and 95 K, are analyzed in terms of the known crystal structure coordinates of the chromphores [3]. It is shown that the shapes of the dichroic ratio spectra of C-PC trimers oriented in PVA films coincide quite well and are of similar quality to those obtained with single crystals [18]. These results are compared to the linear dichroism characteristics of the larger *Nostoc* sp. PC dodecamer for which X-ray crystallographic data are presently not available. Within the wavelength region of 520 nm – 680 nm (PC absorption band), the LD and absorption spectra of the *M. laminosus* trimer and *Nostoc* sp. dodecamer are very similar in shape and magnitude, suggesting that the orientation of the phycobilin chromophores is similar in both systems, and that neither the presence of linker polypeptides nor the state of aggregation beyond the trimers has any noticeable influence on the LD spectra.

It has been suggested that two of the chromophores ($\alpha 84$ and $\beta 84$) in the C-PC trimers of *M. laminosus* are coupled by pairwise exciton interactions [6,7]. The feasibility of using stretched PVA film linear dichroism spectra to differentiate between this exciton coupling model and a model in which the transition moments of all three chromophores are essentially independent, is explored.

## Materials and Methods

*Protein Complexes*

*Nostoc* sp. (strain MAC, Paris Culture Collection No. 8009) cells were grown in cool white fluorescent light (F48PF17/CW Power Groove, General Electric, Stamford, CT; light intensity 8 $W/m^2$), and the PC and phycoerythrin (PE) fractions were isolated from the PBsomes as described elsewhere [19,20]. For *Nostoc* sp. cells grown in white light, the PC component within the intact PBsome is in the hexameric aggregation state. However, upon isolation, which includes centrifugation in gradients containing 0.1 M potassium phosphate buffer at pH 5.0, the PC fraction of the PBsomes forms dodecameric aggregates without apparent change in conformation [19].

Phycobilisomes were isolated from *Mastigocladus laminosus* as described for *Nostoc* sp. [20], except that all solutions contained 0.9 M potassium phosphate. The PBsomes were dissociated by a 2 h dialysis against multiple changes of 5 mM potassium phosphate buffer (pH 7.0) containing 0.02% sodium azide and 1 mM phenylmethylsulfonyl fluoride. The dialysate was centrifuged for 30 min at 17000 rpm in a Sorvall SS-34 rotor centrifuge (DuPont-Sorvall, Wilmington, DE), and the supernatant was then loaded on a Mono Q column and chromatographed on a Pharmacia fast performance liquid chromatography system (Pharmacia-LKB Biotechnology, Piscataway, NJ). The column was developed with a linear gradient of potassium phosphate (5 mM to 1 M). Fractions greatly enriched in PC trimer were pooled, dialyzed extensively against 5 mM potassium phosphate (pH 7.0) and loaded back onto the Mono Q column. The column was again developed with a linear gradient of potassium phosphate from 5 mM to 1 M. Several fractions which contained only PC trimer (determined by fluorescence and absorption spectral analysis, as well as by sedimentation and sodium dodecyl sulfate-polyacrylamide gel electrophoresis) were pooled and used for the spectroscopic analysis detailed below.

*Poly(vinyl alcohol) films*

The PC or PE preparations, all in 0.1 M potassium phosphate buffer (pH 5.0) were added to a solution of 20% (w/v) poly(vinyl alcohol) (Elvanol 71–30, Du Pont de Nemours, Wilmington, DE) in 50 mM Tris-HCl buffer solution (pH 5.0). The viscous mixture was poured into a Petri dish and allowed to air-dry at ambient temperature. The resulting films had a thickness of about 0.3 mm, and 5 mm wide strips were cut and mounted on a laboratory-built stretcher. Typically,

films were stretched by factors of up to 2.2. The degree of stretching was quantified by placing two dots about 1 cm apart and by measuring the distance between the dots as a function of the degree of stretching. The stretching ratio ($n$) was defined as the ratio of the distances between the dots after and before stretching.

*Linear dichroism*

The linear dichroism apparatus was home-built and consisted of the following components: a 150 W Cermax xenon lamp (ILC Technology, Sunnyvale, CA), a 0.2 m J&Y monochromator with a holographic grating (Instruments SA, Metuchen, NJ), a 50 kHz photoelastic modulator (Model PM3, Hinds International, Portland, OR), a photomultiplier tube whose output current was kept constant (as a function of wavelength) by an electronic feedback circuit, and a lock-in amplifier tuned to the 100 kHz oscillations of the linear dichroism signal. A more detailed description of the apparatus may be found elsewhere [21]. The LD system was calibrated using a linear polarizing crystal as described by Breton et al. [22]; all LD values reported here are in absolute units unless noted otherwise. The LD apparatus was also modified to serve as an absorption spectrophotometer in experiments in which comparisons of linear dichroism and absorption spectra were of critical importance.

The linear dichroism is defined as follows:

$$\mathrm{LD} = A_{\parallel} - A_{\perp} \tag{1}$$

where $A_{\parallel}$ and $A_{\perp}$ denote the absorbances measured with the electric vectors ($\mathbf{E}_{\parallel}$, $\mathbf{E}_{\perp}$) of the light oriented either parallel or perpendicular relative to the stretching direction, respectively. The reduced linear dichroism, $R$, is defined by $R = \mathrm{LD}/A$, where $A$ is the isotropic absorption. The polarization ratio $P = A_{\parallel}/A_{\perp}$ is related to $R$ by the following expression:

$$P = \frac{1-R}{2R+1} \tag{2}$$

*Low-temperature experiments*

The low-temperature experiments were performed utilizing a gas flow-cooled cryogenic work station (Model RC 152, Cryo Industries, Salem, NH).

## Results and Discussion

*Modes of orientation and definition of directions of polarization*

The direction of the propagation (**X**), and orientations of the electric field vectors of the polarized light relative to the stretching directions (**S**) of the PVA films are shown in Fig. 1. The longest dimensions of the protein complexes, similar to the preferred modes

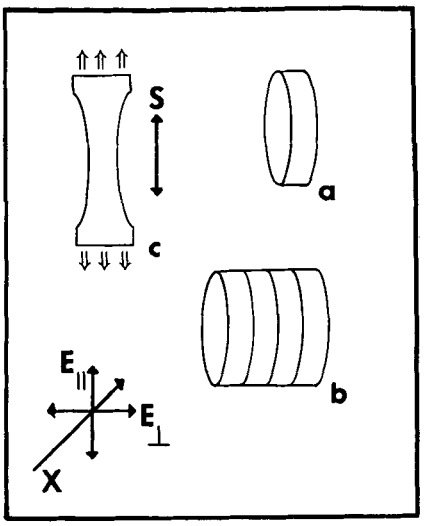


Fig. 1. Schematic representation of orientations of different particles in stretched PVA films: (a) trimeric disk, (b) dodecameric disk stack, (c) stretched PVA film, where **S** is the direction of stretch. **X** is the propagation direction of the incident plane polarized light, which is perpendicular to the plane of the PVA film and to **S**; $E_{\parallel}$ and $E_{\perp}$ are the polarization directions of the electric field vectors of the linearly polarized light, respectively.

of orientation of molecules of various shapes [23,24], tend to orient with their longest dimensions parallel to **S**, the direction of elongation in the stretched films. The mode of orientation of protein complexes derived from PBsomes is similar in PVA films and in squeezed gelatin gels [9,25]. Single disks with dimensions of those of the PC trimers (110 Å × 30 Å [2]), and stacks of up to four disks, tend to align themselves as shown in Fig. 1a and 1b, respectively; aggregates of six or more disks tend to orient in a rod-like fashion with their axes tending to be parallel to **S** [9]. The dimensions of the PC dodecamer should be about 110 Å × 120 Å, and it seems reasonable to assume that it should align itself as a cylinder with its axis parallel to **S**, although the opposite (disk-like) mode of orientation is observed in PVA films (Fig. 3). It is interesting to note that in 10% gelatin/90% water gels the PC dodecamers also orient in the same fashion as disk-like trimers, while stacks of six discs orient like rods, as expected [9]. Thus, the disk-like behavior of the PC dodecamer in gels (and probably in PVA films as well) is not likely to be due to the degradation of these higher aggregates to trimers, since stacks of six disks appear to be stable in the gels. The reasons for the unexpected modes of orientation of the intermediate-size PC dodecamers either in PVA films or in gels are not known at this time.

*Linear dichroism spectra*

The LD and absorption spectra of oriented *M. laminosus* PC trimers in stretched PVA films at room temperature (296 K) and at 95 K, are shown in Figs. 2a

and 2b, respectively. The baselines of the LD spectra were originally skewed, and were corrected for this effect by subtracting a similarly skewed baseline from a stretched control (without PC trimer) PVA film. The absorption spectrum at 95 K is somewhat better defined than at room temperature; the maximum is at 618 nm (same as at 296 K), with shoulders near 577 and 633 nm. The LD spectrum is also sharper at 95 K than at room temperature; a prominent positive LD peak is evident at 634 nm (636 nm at room temperature), and negative LD maxima are observed at 560 and 608 nm.

In *Nostoc* sp. PBsomes isolated from cells grown in white light, PC is found in the hexameric aggregation state; however, in pH 5.0 buffers used in the purification protocol, the PC aggregates to dodecamers [19]. The absorption and LD spectra of *Nostoc* sp. PC dodecamers in stretched PVA films at room temperature and at 95 K are shown in Figs. 3a and 3b, respectively. Both the absorption and LD spectra are similar to the ones shown for the *M. laminosus* PC trimer in Fig. 2. The absorption maximum is located at 622 nm at 296 K, and is slightly red-shifted to 628 nm at 95 K; a shoulder is evident at 570–575 nm. The positive LD maximum occurs at 635 nm at 95 K (639 nm at 296 K), and well-defined minima are observed at 560 and 608 nm at the lower temperature, while at room temperature the minimum is situated at 603 nm.

Both the absorption and LD spectra of *Nostoc* sp. PC dodecamers are similar to the corresponding spectra of the *M. laminosus* PC trimers in terms of the shapes of the absorption and LD spectra, and the location of the LD maxima and minima. These observations suggest that the orientations of the phycocyanobilin chromophores in *Nostoc* sp. are not too different from those in *M. laminosus*, for which the crystallographic structure and atomic coordinates are known [2,3].

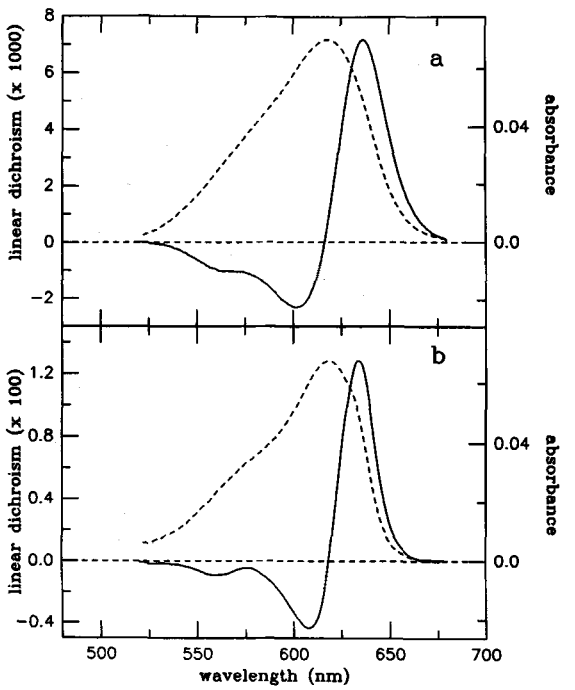


Fig. 2. Linear dichroism (———) and absorption (— — —) spectra of *M. laminosus* PC trimer oriented in a stretched PVA film ($n = 2.0$) at (a) ambient temperature and (b) 95 K.

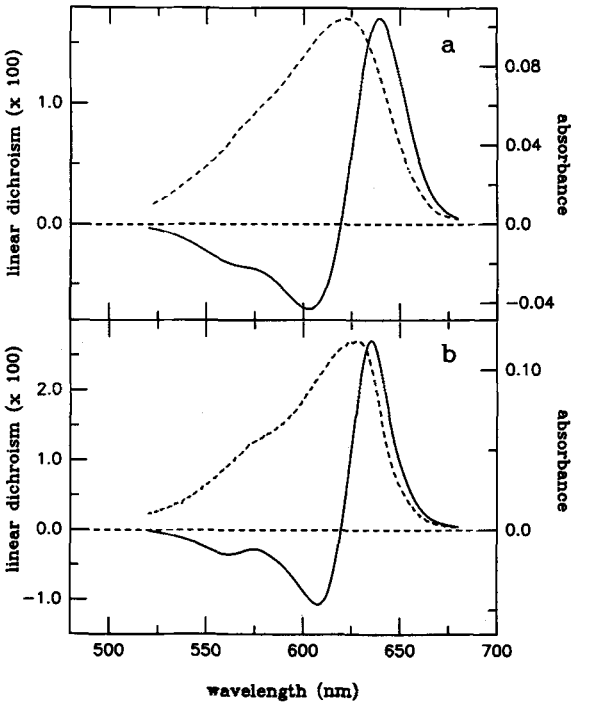


Fig. 3. Linear dichroism (———) and absorption (— — —) spectra of *Nostoc* sp. PC dodecamer oriented in a stretched PVA film ($n = 2.0$) at (a) ambient temperature and (b) 95 K.

*Degree of orientation as a function of n*

The magnitudes of the reduced linear dichroism signals (LD measured from the maximum at 636 to the minimum at 602 nm) of *M. laminosus* PC trimers, embedded in PVA films as a function of the stretching factor, $n$, are shown in Fig. 4. For comparison, a similar set of results is shown with oriented PE trimers derived from *Nostoc* sp. embedded in the same type of PVA film (Fig. 4); in the case of PE trimers, the LD spectrum is similar in shape to that of the PC trimers, but the LD maximum and minimum occur at 572 and 543 nm, respectively (data shown in Ref. 9). The reduced linear dichroism values plotted in Fig. 4 were evaluated by taking into account the decrease in absorbance of the sample as a function of increasing $n$.

For both samples, the magnitude of the reduced LD signal increases rapidly with increasing $n$ at low values of $n$, then exhibits a downward curvature, tending towards saturation, at higher values of $n$. A number of different workers have considered theoretically the forms of orientation functions which could account for

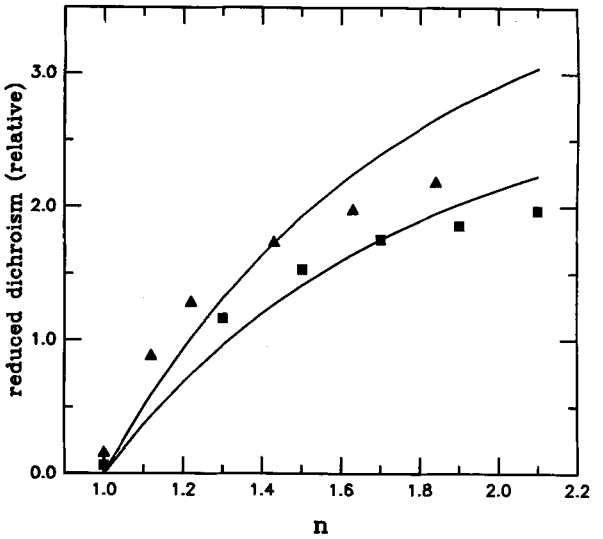


Fig. 4. Relative LD signal for *M. laminosus* PC trimer (▲) and *Nostoc* sp. PE trimer (■) oriented in PVA film at room temperature as a function of $n$, the stretching factor. The magnitudes of the LD signals were determined from the minimum at 602 nm to the maximum at 636 nm for the *M. laminosus* PC trimer, and from the minimum LD at 543 nm to the maximum at 572 nm for the *Nostoc* sp. PE trimer. These values were corrected for the changes in film thickness. (———)····· two plots of the Ganago et al. [14] orientation function (Eqn. 4), adjusted to provide the best possible fits to the two sets of experimental data points.

the degree of orientation of molecules and rod- or disk-shaped objects subjected to uniaxial stretching or compression forces [14,15,23,24,26]. Ganago et al. [14] considered a model in which a sample containing disk- or rod-like objects is extended along one axis and compressed along the other two perpendicular directions; in the case of rod-shaped particles, it was shown that the dependence of the calculated orientation function on $n$ is similar to the one calculated previously by Tanizaki for molecules embedded in stretched PVA films [27]. The dependence of the LD signal of disk-like objects on $n$ has the following form [14]:

$$\mathrm{LD} = (1/4)A\{3\cos^2\theta - 1\}\{3L(n) - 1\} \tag{3}$$

where the orientation function $L(n)$ is given by:

$$L(n) = \frac{1}{n^3 - 1}\left\{-1 + \left(\frac{n^3}{n^3 - 1}\right)^{1/2} \ln\left[n^{3/2} + (n^3 - 1)^{1/2}\right]\right\} \tag{4}$$

The angle $\theta$ defines the inclination of the transition dipole moments with respect to the normal to the plane of the disks. The sign of the function $\{3L(n) - 1\}$ is negative; thus, the sign of the LD signals is positive for $\theta > 54.7°$, and negative for $\theta < 54.7°$.

Two plots of the function $\{3L(n) - 1\}$, each normalized as closely as possible to the experimental PC and PE data points, are plotted in Fig. 4 (solid lines). It is evident that the experimental data points tend to level off with increasing $n$ much faster than predicted from the form of the orientation function. One reason for the poor fit may be that the two dimensions perpendicular to the stretching direction S do not contract equally upon stretching of the PVA film. Another may be that the flat disks respond to the compression of the plane perpendicular to the stretching direction and therefore align themselves nonrandomly around the direction of stretch. Furthermore, some orientational anisotropy already develops when the films are first dried. For example, in an unstretched film containing PC trimers, an LD signal about 7% of the maximum value (measured for $n = 2$) was observed; thus, the mounting of the film in the stretcher most likely results in some stretching giving rise to a small orientation of the PC trimers. For any of these reasons, the dependence of the observed LD signals on n could be different from the one predicted by Eqn. 3, which embodies a pure uniaxial orientation model. Van Amerongen et al. [15] proposed a different orientation function which was derived on the basis of the following model: (a) elongation along one direction, (b) contraction in one of the perpendicular directions and constant dimensions along the third orthogonal direction, and (c) constant volume during deformation; however, this orientation function did not provide a better fit to the experimental results (data not shown). Obviously, the mode of alignment of the PC and PE protein complexes in stretched PVA films cannot be accounted for by these simple orientation models. A further consideration of this topic is beyond the scope of this work.

*Comparisons of LD spectra of PC trimers oriented in stretched PVA films with LD spectra obtained using single crystals [18]*

Schirmer and Vincent [18] obtained the polarization ratio, $P$, of thin single crystals of PC trimers derived from *M. laminosus* by measuring their optical spectra parallel and perpendicular to the $C_3$ symmetry axis (which is parallel to the optic axis ($c$)) using linearly polarized light. There are two trimers per unit cell which are related to one another by a $2_1$ screw axis oriented parallel to $c$. In their case, the polarization ratio is defined as $P = A_{\parallel c}/A_{\perp c}$. It is interesting to determine if the wavelength dependence of this quantity is similar to the wavelength dependence of our $P$ values (Eqn. 2) obtained with isolated PC trimer discs oriented in stretched PVA films.

The $P$ ratios of PC aggregates derived from *M. laminosus* and *Nostoc* sp. oriented in stretched PVA films at room temperature and at 95 K are compared to the dichroic ratio measured by Schirmer and Vincent using single crystals of PC trimers in Fig. 5. At room temperature (Fig. 5a), the magnitude of $P$ is smaller throughout the entire wavelength range in the case of the *M. laminosus* trimers embedded in the

PVA films than in the PC crystals; while the $P$ ratio spectra of the PC-PVA film and PC-crystal resemble one another, the structure in the PVA films is much less pronounced. At 95 K, the magnitude of the $P$ ratios in the PC-PVA samples increases and there is a sharpening of the structure, which is now remarkably similar to the polarization ratio spectrum in the PC crystals at ambient temperatures (Fig. 5b), except for the rise in the $P$ values above 645 nm in the film; this latter effect appears to be due to the smaller tilt angle of the transition dipole moments of the longest-wavelength absorbing pigment forms with respect to the $C_3$ symmetry axis (see below).

The $P$ ratios for *Nostoc* sp. dodecamers embedded in PVA films are somewhat higher than those of our *M. laminosus* preparations, but the wavelength dependence is similar. The resemblance of the polarization ratios between *Nostoc* sp. dodecamers, and the PC trimers of *M. laminosus* in PVA films and in single crystals suggests that the orientation of the chromophores in the *Nostoc* sp. PC proteins, for which the crystal structure is unknown, is similar to the orientation of the chromophores in PC trimers of *M. laminosus*, whose crystal structure is known [2,3].

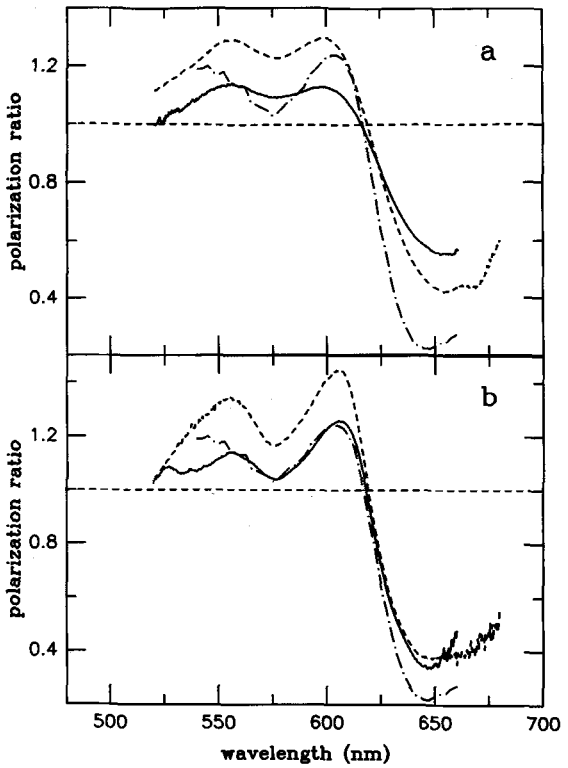


Fig. 5. Polarization ratio ($A_\perp / A_\parallel$) spectra calculated from the data in figures 2 and 3, using Eqn. 2. (a) *M. laminosus* PC trimer (———) and *Nostoc* sp. PC dodecamer (— — —) oriented in PVA film at room temperature. (b) *M. laminosus* PC trimer (———) and *Nostoc* sp. PC dodecamer (— — —) oriented in PVA film at 95 K. In both (a) and (b), the polarization ratio for crystallized *M. laminosus* PC trimers (–·–·–), taken from Ref. 18, is also shown.

The absolute polarization ratios $P$ (Eqn. 2) in single C-PC crystals and and C-PC trimers in stretched PVA films at room temperature are compared to one another in Fig. 5a. In general, these $P$ values are not expected to be identical to one another because of a different symmetry and imperfect degrees of orientation in the PVA films. However, in this case, the crystal space group is $P6_3$, and the crystal unit cell contains two trimers related to one another by a $2_1$ screw axis parallel to the crystal symmetry ($c$) axis; the symmetry axis of the trimers is parallel to this direction [18]. Thus, the observed lower $P$ ratio in the PVA films with uniaxial symmetry is reasonable. At the lower temperature (Fig. 5b), the experimental $P$ ratios are higher than those at room temperature; the single crystal $P$ ratios of Schirmer and Vincent [18], presumably measured at ambient temperatures, is also shown for reference.

*Analysis of LD spectra in terms of models of non-interacting chromophores and pairwise exciton interactions*

The *M. laminosus* C-PC trimers contain two types of polypeptide, $\alpha$ and $\beta$, to which are attached three different types of phycocyanobilin chromophores $\alpha$84, $\beta$84 and $\beta$155. The orientation of each of the three chromophores in crystals of the C-PC trimers has been determined at high resolution (2.1 Å) by X-ray structure analysis [3]. The $(\alpha\beta)_3$ trimer consists of $\alpha\beta$-monomers in a ring-like structure in a head-to-tail arrangement; the $C_3$ axis passes through the center of the ring and is perpendicular to its plane. The $\beta$155 chromophore extends almost parallel to the **c** axis, while the $\alpha$84 chromophore of one monomer unit is in close proximity (2.1 nm) to the $\beta$84 chromophore of the neighboring monomer unit. Using various spectroscopic methods, and based on the known X-ray structure of C-PC, Mimuro et al. have concluded that the $\beta$155 and $\alpha$84 phycobilins are the sensitizing ('s') chromophores, while $\beta$84 is the fluorescence-emitting ('f') chromophore [4,5]. Mimuro et al. [4] have shown that the overall absorption spectrum of the C-PC trimers of *M. laminosus* in buffer solution can be reasonably well approximated by a sum of the individual $\beta$155, $\alpha$84 and $\beta$84 absorption spectra. These individual absorption spectra are reproduced in Fig. 6a and are characterized by absorption maxima at 594, 618 and 624 nm, respectively.

Sauer and Scheer [7] have proposed that the $\beta$84 and $\alpha$84 chromophores are coupled by exciton interactions because of their close proximities and favorable mutual orientations. In that case, the C-PC trimer absorption spectrum should be a superposition of an uncoupled $\beta$155 monomeric absorption spectrum, and the two exciton absorption bands resulting from the coupling of the $\alpha$84 and $\beta$84 components; however, the absorption maxima of these two excitonic compo-

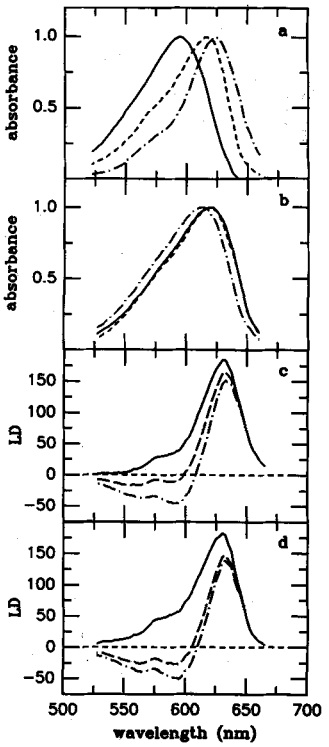


Fig. 6. (a) Normalized absorption spectra of each *M. laminosus* PC chromophore in its protein environment deduced by Mimuro et al. [4]: $\beta$155 (———), $\alpha$84 (— — —), and $\beta$84 chromophore (–·–·–·–·–). (b) Absorption spectra of C-PC trimers constructed from the normalized absorption spectra of the individual components shown in (a), assuming that all oscillator strengths are approximately equal to one another. (–·–·–·–·–)····· wavelength positions of individual spectra as deduced by Mimuro et al. [4] and shown in (a); (– – – – – –)····· absorption spectrum calculated by red-shifting the individual absorption components shown in (a) as follows: $\beta$84 by 5 nm, and $\alpha$84 and $\beta$155 by 7.5 nm. The experimental absorption spectrum of *M. laminosus* trimers at room temperature is also shown (———). (c) Simulated linear dichroism spectra constructed from the data in Table I (*molecular* model) and Eqn. 5, using different values of the transition dipole moment $\|\mu_{\beta155}\|^2$: (———) 107, (— — —) 160, and (–·–·–·–) 200. (d) Simulated linear dichroism spectra constructed from the data in Table II (*exciton model*) and Eqn. 8, utilizing different values of $\|\mu_{\beta155}\|^2$: (———) 107, (— — —) 200, and (–·–·–·–) 225.

nents, because of a relatively small exciton splitting, are not expected to differ significantly from those of the individual $\alpha$84 and $\beta$84 monomers [7]. Because the two interacting chromophores are spectroscopically non-degenerate, the interaction energy will be even smaller (42 $cm^{-1}$, K.S., unpublished calculations) than the value (56 $cm^{-1}$) calculated based on degenerate chromophore energy levels [7].

In Sauer and Scheer's simple pairwise exciton model, the transition moment vectors of the two coupled chromophores are vectorially added and subtracted from one another to produce two new exciton transition moment directions, which may be different from those of the uncoupled transition moment vectors. The *exciton-coupled* transition moment directions can be calculated from the known coordinates of the chromophores, and from a knowledge of the orientations of the individual molecular transition moment directions relative to the framework of the three chromophores. These latter directions have been recently estimated by two different methods: (1) Schirmer et al. (Ref. 3, Table 9) obtained the directions of the transition dipole moments, to a first approximation, by fitting the conjugated portion of each chromophore to a line by a least-squares method; (2) the dipole transition moment ($\mu$) magnitudes and directions were calculated from the coordinates of the chromophores [3] and the transition monopoles evaluated by Scharnagl and Schneider (personal communication). These parameters, obtained by the latter method, are listed for all three chromophores in Table I. Values of the calculated squared transition dipole moments ($\|\mu\|^2$), the angle $\theta$ between the individual transition moments and the symmetry (**c**) axis of the trimers, and the factor $\{3\cos^2\theta - 1\}$, are also provided.

The sensitivity of the linear dichroism spectra of C-PC trimers to the orientations of the transition dipole moments of the oriented chromophores might, in principle, provide information favoring either the molecu-

TABLE I

*Transition moment magnitudes (debyes) of chromphores along the c axis, and along the two perpendicular directions (a and b) in M. laminosus C-PC trimers, evaluated from the transition monopole calculations of Scharnagl and Schneider (personal communication), and the known crystal coordinates [3]*

$\|\mu_i\|$, absolute value of transition dipole moments. $\theta_i$, angle between transition dipole moment and *c* ($C_3$ symmetry axis of C-PC trimers).

| Axis | $\beta$155 | | | $\alpha$84 | | | $\beta$84 | | |
|---|---|---|---|---|---|---|---|---|---|
| | 1 | 2 | 3 | 1 | 2 | 3 | 1 | 2 | 3 |
| *a* | 4.23 | 1.69 | −5.92 | −5.51 | 14.2 | −8.68 | −3.35 | 11.86 | −8.51 |
| *b* | −4.39 | 5.86 | −1.47 | −13.2 | 1.83 | 11.4 | −11.8 | 2.98 | 8.78 |
| *c* | 8.34 | 8.34 | 8.34 | 3.18 | 3.18 | 3.18 | 7.11 | 7.11 | 7.11 |
| $\|\mu_i\|^2$ | 107 | | | 215 | | | 200 | | |
| $\theta_i^0$ | 36.2 | | | 77.5 | | | 59.8 | | |
| $3\cos^2\theta_i - 1$ | 0.955 | | | −0.859 | | | −0.242 | | |
| Sign of LD | negative | | | positive | | | positive | | |

lar or the exciton-coupled model. In an attempt to determine which of these two models can better describe the observed LD spectra of oriented C-PC trimers, we have simulated the LD spectra using a *molecular* model (no exciton interactions between any of the chromophores), and an *exciton* model (pairwise interaction between $\alpha 84$ and $\beta 84$ chromophores [7]). Relative values of simulated LD spectra were calculated according to equation [1], assuming that the absorbance $A$ of each molecular or excitonic band is proportional to $\| \mu \|^2$, and that the sign of the function $\{3L(n) - 1\}$ is negative.

*The molecular model*

In the molecular model, the LD spectra were simulated by adding the contributions of all three non-interacting chromophores using the orientation angles $\theta$ given in Table I and the expression:

$$\mathrm{LD(molecular)} = \sum_i \mathrm{constant} * \left(\| \mu_i \|^2\right)(f_i) \times \left(3\cos^2\theta_i - 1\right) \quad (5)$$

where the subscript i denotes the individual contributions of the three chromophores. The $f_i$, or $f_{\beta 155}$, $f_{\alpha 84}$, and $f_{\beta 84}$ terms, are the normalized absorption spectra of the $\beta 155$, $\alpha 84$ and $\beta 84$ chromophores, respectively, adapted from Mimuro et al. [4] (Fig. 6a), which provide the wavelength dependence of the simulated LD spectra. Mimuro et al. [4] showed that the molar extinction coefficients of each of the three chromophores are approximately equal to one another (within $\pm 10\%$). In Fig. 6b, the simulated absorption spectrum (–·–·–·–), estimated by summing the three $f_i$ spectra in Fig. 6a, is compared to the experimentally measured absorption spectrum (solid line). Since these spectra do not coincide, it was necessary to red-shift the individual (Mimuro et al. [4]) $f_{\beta 84}$ spectrum by 5 nm and the $f_{\beta 155}$ and $f_{\alpha 84}$ spectra by 7.5 nm, in order to obtain a good approximation (dashed line, Fig. 6b) to the experimentally obtained absorption spectrum; the difference between the simulated absorption spectrum and the experimental absorption spectrum does not exceed approx. 4% in the 550–650 nm region (data not shown). Since the Mimuro et al. [4] spectra ($f_i$) were derived from experimental monomer absorption spectra, the red-shifting of these individual spectra to simulate the PC trimer absorption spectrum is attributed to differences in the aggregation state, rather than to specific effects introduced by the PVA films. In fact the absorption spectra and absorption maxima (618 nm) are the same in buffer solution and in the PVA films.

Another model of the absorption spectra of the individual *M. laminosus* PC chromophores is that of Sauer et al. [6]; the spectral widths and shapes are equal to one another in this model, but the molar extinction coefficient of the $\beta_{84}$ is about 35% smaller than that of the $\beta_{155}$ chromophore, in contrast to the Mimuro et al. [4] model in which these values are almost equal to one another. Therefore, an upward revision of the molar extinction coefficient of the $\beta_{84}$ as well as red-shifts in the absorption spectra of the three chromophores (12.5, 10 and 7.5 nm for the $\beta_{155}$, $\alpha_{84}$ and $\beta_{84}$ chromophores, respectively) were required to obtain a reasonable approximation of the experimental absorption spectrum (data not shown). Upon the introduction of these parameters, the Sauer et al. spectra could also have been used to simulate the absorption spectra of the *M. laminosus* trimer; however, the Mimuro et al. [4] spectra were employed to illustrate the methods of calculation of linear dichroism spectra. The individual red-shifted $f_i$ functions (Fig. 6b) were used in all of the LD calculations with the individual absorbances $A_i \propto \|\mu_i\|^2 f_i$.

*The exciton model*

In the exciton model, the following procedure was used:

(1) The directions of the three components of the (+) and (−) exciton transition dipole moments arising from the coupling of the $\alpha 84$ and $\beta 84$ chromophores

TABLE II

*Amplitudes of exciton transition dipole moment vectors*

$\mu_\pm(1) = \mu(1\alpha 84) \pm (2\beta 84)$; $\mu_\pm(2) = (\mu 2\alpha 84) \pm \mu(3\beta 84)$; $\mu_\pm(3) = \mu(3\alpha 84) \pm (1\beta 84)$.

| Axis | $\mu_-(1)$ | $\mu_-(2)$ | $\mu_-(3)$ | $\mu_+(1)$ | $\mu_+(2)$ | $\mu_+(3)$ |
|---|---|---|---|---|---|---|
| a | −12.28 | 16.06 | −3.77 | 4.49 | 4.02 | −8.51 |
| b | −11.44 | −4.92 | 16.41 | −7.23 | 7.50 | −0.28 |
| c | −2.78 | −2.78 | −2.78 | 7.28 | 7.28 | 7.28 |
| $\|\mu_\pm\|^2$ | 290 | | | 125 | | |
| $\theta^0_\pm$ | 99.4 | | | 49.5 | | |
| $3\cos^2\theta_\pm - 1$: | −0.92 | | | 0.265 | | |
| Sign of LD | positive | | | negative | | |

were evaluated using the data in Table I, according to the expression:

$$\mu_{\pm} = (1/\sqrt{2})\{\mu_{1\alpha 84} \pm \mu_{2\beta 84}\} \quad (6)$$

where the indices 1 and 2 refer to the chromophores in different monomer units of the trimer according to the known coupling scheme [3,7]. Similar expressions were used to calculate $\boldsymbol{\mu}_{\pm}$ for the coupled $2\alpha 84 - 3\beta 84$, and $3\alpha 84 - 1\beta 84$ chromophores (Table II). Since the amplitudes of the $\alpha 84$ and $\beta 84$ transition dipole moments are slightly different from one another (Table I), the angle between the two excitonic transition dipole moments, calculated from the data in Table II, is 87.8° rather than 90°.

(2) The magnitudes of the individual dipole strengths of the two exciton components were calculated according to:

$$\|\boldsymbol{\mu}_{\pm}\|^2 = (1/2)\{\|\boldsymbol{\mu}_{\alpha 84}\|^2 + \|\boldsymbol{\mu}_{\beta 84}\|^2 \pm 2\boldsymbol{\mu}_{\alpha 84}\cdot\boldsymbol{\mu}_{\beta 84}\} \quad (7)$$

(3) The $\beta 155$ chromophore was not coupled to any of the others and the directions and dipole strengths were taken directly from Table I; however, because this theoretical value appears to be too small, calculations were also performed with two larger values of $\|\boldsymbol{\mu}_{\beta 155}\|^2$ (see below).

(4) Linear dichroism spectra were constructed according to the following sum:

$$\begin{aligned}\text{LD(exciton model)} = \text{constant} \\ \cdot\{&\|\boldsymbol{\mu}_{\beta 155}\|^2 f_{\beta 155}(3\cos^2\theta_{\beta 155} - 1) \\ &+ \|\boldsymbol{\mu}_{-}\|^2 f_{\alpha 84}(3\cos^2\theta_{-} - 1) \\ &+ \|\boldsymbol{\mu}_{+}\|^2 f_{\beta 84}(\cos^2\theta_{+} - 1)\}\end{aligned} \quad (8)$$

where the angles $\theta_{-}$ and $\theta_{+}$ denote the angles between the $C_3$ axis and the (−) and (+) exciton transition dipole moments.

The energies ($E_{\pm}$) of the two exciton components ($E_{\pm} \approx E \pm V_{12}$) depend on the sign of the interaction term $V_{12}$, where $E$ is the averaged energy of the two interacting monomers, and:

$$\begin{aligned}V_{12} = &(\boldsymbol{\mu}_{\alpha 84}\cdot\boldsymbol{\mu}_{\beta 84})\mathbf{R}_{12}^{-3} \\ &-3(\boldsymbol{\mu}_{\alpha 84}\cdot\mathbf{R}_{12})(\boldsymbol{\mu}_{\beta 84}\cdot\mathbf{R}_{12})\mathbf{R}_{12}^{-5}\end{aligned} \quad (9)$$

$\mathbf{R}_{12}$ being the vector joining the two centers of the interacting chromophores. According to the data provided by Schirmer et al. (Ref. 3, Table 10), the sign of $V_{12}$ is negative, and thus we conclude that the (+)-exciton has the lower energy.

Since the absorption maxima of the two excitonic components are predicted to be quite close to those of the $\alpha 84$ and $\beta 84$ monomers [7], the (−)- and (+)-exciton component absorption spectra were assumed to be the same as those of the $\alpha 84$ and the $\beta 84$ chromophores, respectively. The individual contributions of the $\beta 155$, $\beta 84$, and $\alpha 84$ chromophores to the overall absorption spectrum of the PC trimer are not known exactly [4]; the values of the absorption coefficients, especially the relative value of $\|\mu_{\beta 155}\|^2$, significantly affect the appearance of the LD spectra estimated via Eqn. 5 or Eqn. 8.

Typical examples of such simulated LD spectra according to the *molecular* and *exciton* models, using the coordinates in Tables I and II, are depicted in Figs. 6c and 6d, respectively.

*Comparisons between simulated and experimental LD spectra*

In the exciton model, the $\boldsymbol{\mu}_{-}$ transition contributes strongly to the absorbance in the plane of the trimer disks and perpendicular to the **c** axis; since the value of the orientation factor ($3\cos^2\theta - 1$) is large and negative in sign (Table II); this exciton component therefore contributes a strong positive LD signal whose shape resembles the absorption spectrum of the $\alpha 84$ chromophore. The value of the orientation factor of the $\boldsymbol{\mu}_{+}$ component is +0.265, and thus it contributes a negative LD signal in the long wavelength region of the spectrum. In comparing the values of the orientation factors in Tables I and II, it is evident that the exciton interaction between $\alpha 84$ and $\beta 84$ tilts the transition moment of the lower energy $\boldsymbol{\mu}_{+}$ component closer to the **c** axis (as compared to the lowest energy $\beta 84$ transition moment). The $\beta 155$ chromophores give rise to a larger absorbance parallel to the **c** axis and thus contributes a negative LD signal at the shorter wavelength side of the absorption maximum. The positions of the minima and the maxima in the LD spectra result from the addition of positive and negative LD components; we conclude that the shoulders in the negative LD spectra near 560 nm (Figs. 2 and 3) arise from the differences in the shapes of the $\beta 155$ and $\alpha 84$ absorption bands on the short-wavelength side of the maxima.

Utilizing the theoretical $\|\mu_{\beta 155}\|^2 = 107$ value given in Table I, the LD spectra are positive throughout the entire wavelength region of interest in both cases. However, the experimental results of Mimuro et al. [4] suggest that the molar extinction coefficients of the three separate chromophores are close to one another in value, in contrast to the theoretical results which suggest that the extinction coefficient of the $\beta 155$ chromophore is smaller than that of the other two chromophores by a factor of about 2 (Table I). We have therefore examined the effects of increasing the values of $\|\boldsymbol{\mu}_{\beta 155}\|^2$ on the simulated LD spectra. Two additional examples of simulated LD spectra, utilizing $\|\boldsymbol{\mu}_{\beta 155}\|^2 = 160$ and 200 in the molecular model, or 200 and 225 in the exciton model, are shown in Figs. 6c and

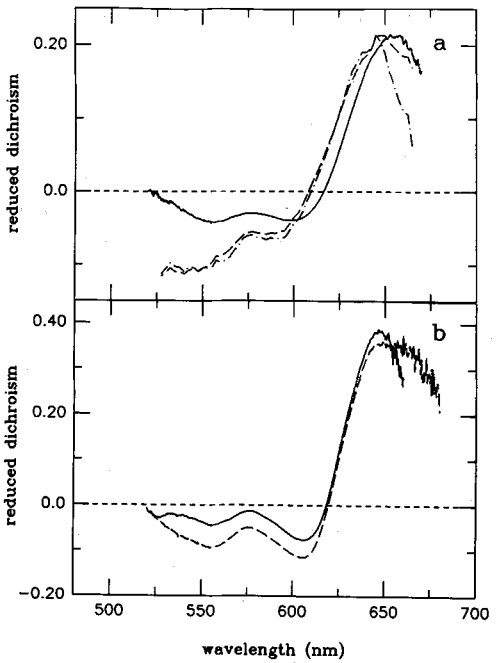


Fig. 7. Simulated and reduced linear dichroism spectra (LD/A) of PC aggregates in stretched PVA films. (a) Room temperature, (———)····· experimental data for *M. laminosus* PC trimer. Simulated spectra: (— — —)····· molecular model, using same data as for the lowest LD curve shown in Fig. 6c; (–·–·–·–)····· exciton model, using same data as for the lowest LD curve shown in Fig. 6d. (b) 95 K, (———)····· experimental data for *M. laminosus* trimer, and (— — —)····· *Nostoc* sp. dodecamer.

6d, respectively. As the relative absorbance of the $\beta 155$ chromophore is increased, a negative LD signal below 600–610 nm manifests itself in the simulated spectra. In the molecular model, with a value of $\| \mu_{\beta 155} \|^2 = 200$, the simulated LD signal is closest in shape and sign to the experimentally measured LD spectrum (Fig. 2a). In the exciton model, a similar resemblance is achieved only if $\| \mu_{\beta 155} \|^2$ is increased to a value of 225 (Fig. 6d). Thus, both the molecular and the exciton models provide reasonably good simulations of the observed LD spectra, but with somewhat different values of the molar extinction coefficients of the $\beta 155$ chromophore relative to those of the $\alpha 84$ and $\beta 84$ chromophores.

The simulated reduced linear dichroism spectra are compared to the LD/A spectrum of the PC-trimers in PVA films at room temperature in Fig. 7a. In these simulations, the $\| \mu_{\beta 155} \|^2$ of 200 and 225 (molecular and exciton models, respectively) were employed which give rise to the simulated LD spectra which most closely resemble the experimental LD spectra (lowest curves in Figs. 6d and 6c). Using these values of $\| \mu_{\beta 155} \|^2$, the two simulated curves closely resemble one another below $\approx$ 650 nm. The long-wavelength cut-off at 670 nm (experimental curve) is dictated by the poor signal/noise ratio beyond this wavelength due to the vanishing absorbance. Comparison of simulated reduced linear dichroism spectra with experimental data (Fig. 7a) is particularly difficult because of inaccuracies in both the numerator and denominator of the calculated LD/*A*. In both the exciton and the molecular models, the magnitude of LD/*A* is predicted to decrease with increasing wavelength beyond 650 nm, this decrease being more pronounced in the exciton model. While such a decrease, which seems to coincide better with the molecular than with the exciton model, is indeed observed in the experimental LD/*A* curve (Fig. 7a), it is not sufficiently well pronounced to differentiate between these two models.

At low temperatures, the decrease at the red edge of the spectrum is also observed in both samples, but comparisons with simulated LD/A spectra are not possible because the lineshapes and widths of the individual chromophore absorption spectra are unknown at 95 K. In the case of *Nostoc* sp. dodecamers (dashed line, Fig. 7b), the decrease in the LD/*A* signal beyond 650 nm at 95 K is less pronounced than in the case of *M. laminosus* trimers.

The simulated LD curves deviate significantly in wavelength position and in shape from the experimental curve below $\approx$ 640 nm; this is a consequence of the lack of knowledge of the individual chromophore absorption spectra. Furthermore, below 550–570 nm, other higher energy transition moments, which have not been taken into account here, may also contribute to the experimental LD and absorption spectra. Such effects may account for the differences between the simulated and experimental reduced linear dichroism spectra in this wavelength region (Fig. 7a).

In summary, the individual chromophore absorption spectra and their molar absorptivities are not sufficiently well characterized at this time to allow for a definite conclusion regarding the applicability of one or the other model. However, these results suggest that a more precise knowledge of the magnitudes of the relative contributions of each of the three chromophores to the overall absorption band in the long wavelength region would indeed allow for a differentiation between the *molecular* and *exciton* coupling models.

## Conclusions

The agreement between the shapes of the simulated and the observed linear dichroism (LD) spectra appears to be better than in the case of the polarization ratio (P) spectra [18]. The sensitivity of the simulated LD spectra to the relative magnitudes of the transition dipole moments of the three chromphores suggests that the LD method can be a useful tool for verifying the orientations and relative magnitudes of transition dipole moments calculated from molecular coordinates, and the possible existence of exciton coupling. At the present time, there is too much uncertainty in

the magnitudes of the relative oscillator strengths of the $\beta$155, $\alpha$84, and $\beta$84 chromophores, in the C-PC trimer of *M. laminosus* to allow for an unambiguous identification of exciton interactions between the $\alpha$84 and $\beta$84 chromophores based on comparisons of predicted and experimentally observed linear dichroism spectra.

In the past, linear dichroism spectra have been utilized predominantly to obtain information about orientation angles of chromophores. These techniques continue to be useful in those cases in which the atomic coordinates are known from X-ray diffraction studies. LD methods can be employed to provide semi-quantitative information on the orientation of transition dipole moments relative to the framework of the pigment molecules and to study the occurrence of exciton interactions.

## Acknowledgements

The authors wish to thank Dr. Scharnagl (Munich) and Prof. Schneider (Erlangen) for providing the results of their transition moment calculations prior to publication. This work was supported by the U.S. Department of Agriculture Grant No. 88-37262-3859 (N.E.G. at New York University) and Grant No. 87-CRCR-1-2318 (B.A.Z., Rutgers University). At Berkeley, this research was supported, in part, by the Director, Office of Energy Research, Division of Energy Biosciences, of the U.S. Department of Energy under Contract No. DE-AC03-76SF00098 (K.S.).

## References

1 Zilinskas, B.A. and Greenwald, L.S. (1986) Photosynth. Res. 10, 7–35.
2 Schirmer, T., Bode, W., Huber, R., Sidler, W. and Zuber, H. (1985) J. Mol. Biol. 184, 257–277.
3 Schirmer, T., Bode, W. and Huber, R. (1987) J. Mol. Biol. 196, 677–695.
4 Mimuro, M., Füglistaller, P., Rümbeli, R. and Zuber, H. (1986) Biochim. Biophys. Acta 848, 155–166.
5 Mimuro, M., Rümbeli, R., Füglistaller, P. and Zuber, H. (1986) Biochim. Biophys. Acta 851, 447–456.
6 Sauer, K., Scheer, H. and Sauer, P. (1987) Photochem. Photobiol. 46, 427–440.
7 Sauer, K. and Scheer, H. (1988) Biochim. Biophys. Acta 936, 157–170.
8 Breton, J. and Vermeglio, A. (1982) in Photosynthesis: Energy Conversion by Plants and Bacteria (Govindjee, ed.), Vol. 1, pp. 153–194, Academic Press, London.
9 Juszczak, L., Geacintov, N.E., Zilinskas, B.A. and Breton, J. (1988) in Photosynthetic Light Harvesting Systems (Scheer, H. and Schneider, S., eds.), pp. 281–292, Walter de Gruyter, Berlin.
10 Gagliano, A.G., Geacintov, N.E. and Breton, J. (1986) Photochem. Photobiol. 43, 551–558.
11 Gagliano, A.G., Breton, J. and Geacintov, N.E. (1986) Photobiochem. Photobiophys. 10, 213–221.
12 Gagliano, A.G., Hoarau, J., Breton, J. and Geacintov, N.E. (1985) Biochim. Biophys. Acta 808, 455–463.
13 Bruce, D. and Biggins, J. (1985) Biochim. Biophys. Acta 810, 295–301.
14 Ganago, A.O., Fok, M.V., Abdurakhmanov, I.A., Solov'ev, A.A. and Erokhin, Yu.E. (1980) Mol. Biol. (USSR) 14, 381–389.
15 Van Amerongen, H., Vasmel, H. and Van Grondelle, R. (1988) Biophys. J. 54, 65–76.
16 Frackowiak, D., Erokhina, L.G., Picard, G. and Leblanc, R.M. (1987) Photochem. Photobiol. 46, 277–285.
17 Frackowiak, D., Fiksinski, K. and Pienkowska, H. (1977) Stud. Biophys. 63, 183–187.
18 Schirmer, T. and Vincent, M.G. (1987) Biochim. Biophys. Acta 893, 379–385.
19 Zilinskas, B.A. and Howell, D.A. (1983) Plant Physiol. 71, 379–387.
20 Troxler, R.F., Greenwald, R.S. and Zilinskas, B.A. (1980) J. Biol. Chem. 255, 9380–9387.
21 Geacintov, N.E., Ibanez, V., Rougee, M. and Bensasson, R.V. (1987) Biochemistry 26, 3087–3092.
22 Breton, J., Michel-Villaz, M. and Paillotin, G. (1973) Biochim. Biophys. Acta 314, 42–56.
23 Michl, J. and Thulstrup, E.W. (1986) Spectroscopy with Polarized Light, VCH Publishers, New York.
24 Nordén, B. (1980) J. Chem. Phys. 72, 5032–5038.
25 Juszczak, L.J., Zilinskas, B.A., Geacintov, N.E. and Breton, J. (1990) in Current Research in Photosynthesis (Baltscheffsky, M., ed.), Vol. 2, pp. 125–128, Kluwer, Dordrecht.
26 Tanizaki, Y. (1959) Bull. Chem. Soc. Japan 32, 75–80.
27 Tanizaki, Y. (1965) Bull. Chem. Soc. Japan 38, 1798–1799.